

Tectonic geomorphology and hydrocarbon induced topography of the Mid-Channel Anticline, Santa Barbara Basin, California

E.A. Keller^{a,*}, Marlene Duffy^a, J.P. Kennett^a, T. Hill^b

^a Department of Earth Science, University of California, Santa Barbara, Santa Barbara, CA 93106, United States

^b Geology Department, University of California, Davis, CA 95616, United States

Received 2 December 2005; received in revised form 15 November 2006; accepted 18 December 2006

Available online 22 December 2006

Abstract

The geomorphology of the western sector of the Mid-Channel Anticline (MCA), Santa Barbara, southern California suggests the actively growing fold is laterally propagating to the west. The presence of fold scarps and cross faults that segment the structure suggests that buried faults that are producing the folding are present at shallow depths. The summit area of the anticline at the Last Glacial Maximum (22 to 19 ka) was probably a small late Pleistocene island. Evidence for presence of the island includes what appears to be terrestrial erosion and is supported by assumption of sea level change and rates of uplift and subsidence.

Pockmarks and domes ranging in diameter from ~10 to 100 m, and several meters deep are present along the crest and flanks of the MCA. These features appear to be the result of hydrocarbon emission. Their formation has significantly modified the surface features, producing simple to complex erosional and/or constructional topography. A large pockmark near the anticline crest dated by two calibrated AMS radiocarbon dates of 25.3 and 36.9 ka continues to emit hydrocarbon gases. We term the topography produced by hydrocarbon emission as Hydrocarbon Induced Topography (HIT).

© 2007 Elsevier B.V. All rights reserved.

Keywords: Active folding; Tectonic geomorphology; Hydrocarbon induced topography

1. Introduction

Fundamental understanding of the growth and development of large, active folds that contain blind (buried) reverse faults is important in the evaluation of the earthquake hazard. It is known that blind faults produce large damaging earthquakes and that these faults commonly have superficial expression as anticline ridges with fold scarps segmented by cross faults (Keller et al., 1998, 1999). On land, geomorphic features that suggest active folding and faulting (and thus earthquake hazard) are often concealed due to surface incision, erosion and deposition

on fold and fault scarps. Thus tectonic geomorphic expression of folding above blind reverse faults is often absent. This hinders understanding of fold growth and the earthquake hazard of blind faults. The Mid-Channel Anticline (MCA), along the Mid-Channel Trend of Nicholson et al. (2006) is a fold for which high-resolution bathymetric data are available. The MCA therefore provides a rare opportunity to document fold morphology.

1.1. Study area

Santa Barbara Basin (Fig. 1) is the modern offshore extension of Ventura Basin. Sedimentary fill in the basin varies from about 8 to 14 km, being thickest in the onshore Ventura Basin (Yeats, 1981, 1983; Eichhubl et al., 2002).

* Corresponding author. Fax: +1 805 893 2316.

E-mail address: keller@geol.ucsb.edu (E.A. Keller).

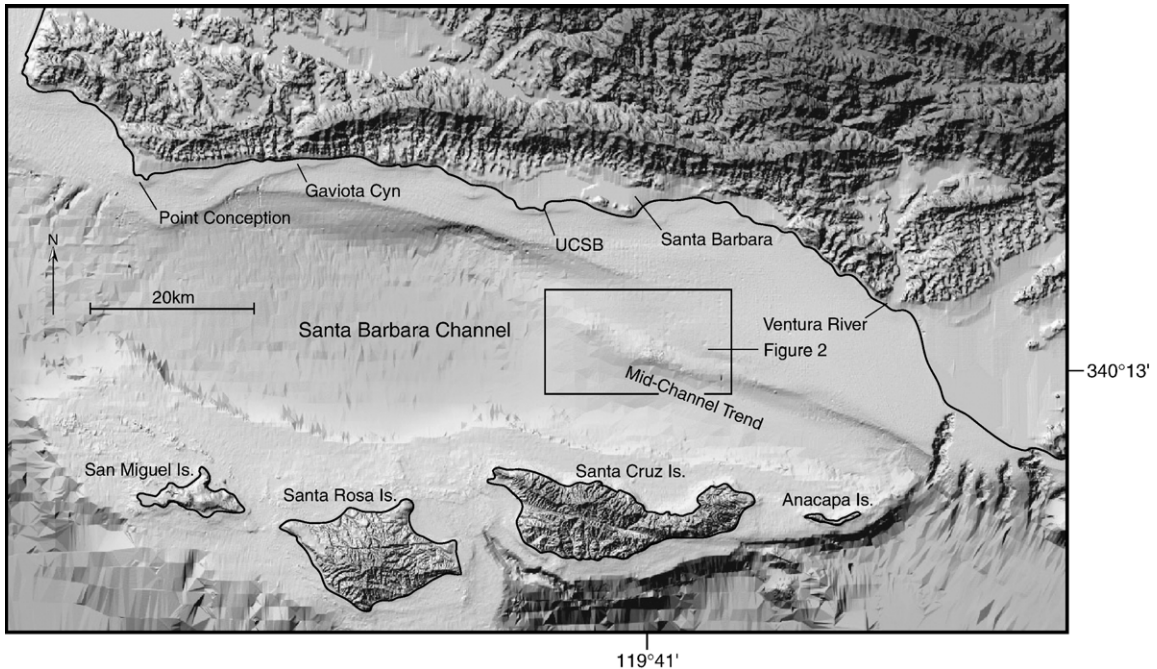


Fig. 1. The Santa Barbara Channel and study area in the central part of the channel. The boxed area is shown on Fig. 2.

Geologic history of the Santa Barbara Basin is marked by Miocene extension and Quaternary shortening (Crowell, 1987). Santa Barbara Basin is the forward part of the southward propagating Santa Barbara Fold Belt formed by Pleistocene shortening south of the Santa Ynez Mountains (Yeats, 1981; Namson and Davis, 1988; Keller and Loaiciga, 1993; Keller and Gurrola, 2000). The offshore Ventura Basin between Santa Barbara and Santa Cruz Island has been inferred to be underlain by a north-dipping blind thrust fault (Shaw and Suppe, 1994; Seeber and Sorlien, 2000; Sorlien et al., 2000; Pinter et al., 2003; Nicholson et al., 2006) that is responsible for shortening and growth of folds.

The MCA is the dominant sea floor structure in the central-eastern section of Santa Barbara Basin. The study area is the westernmost section of MCA, which has produced a topographic high (Fig. 1). The topographic expression of folding at the seafloor is a linear ridge about 7 km wide and 25 km long with local relief of about 100 m. Sedimentary rocks exposed at the crest of MCA are late Pleistocene in age (Sorlien and Kamerling, 1998). The fold is part of the Santa Barbara Fold Belt, which extends from the Santa Ynez Mountains south to Santa Cruz Island (Gurrola and Keller, 1997; Keller and Gurrola, 2000; Keller et al., 2001). The series of roughly east–west folds of the Santa Barbara Basin is forming in response to north–south shortening of about 6 mm/yr (Larson and Webb, 1992), presumably in response to the

left bend, “big bend” of the San Andreas Fault located approximately 80 km to the north of the study area. The MCA is the site of many small earthquakes that define the recent seismicity of Santa Barbara Basin (Sylvester et al., 1970; Henyey and Teng, 1985). Several M_W 2.5 to 3.5 events occurred under the MCA as recently as 2000.

1.2. Purpose and objectives

The purpose of the research on the MCA is to interpret geomorphic data to better understand the topographic development of an active large pristine anticline whose structural origin is controversial. The documentation of geomorphic data may help reduce the uncertainty of structural interpretation based on subsurface geologic and geophysical data. One of the guiding principles of tectonic geomorphology is the application of geomorphic analysis to help assist with the understanding of structural development (Keller and Pinter, 2002).

This investigation has several objectives: 1) to complete a detailed tectonic geomorphic analysis of the MCA to delineate and document topographic features such as fault and fold scarps, and cross faults, as they relate to fold morphology and development; 2) to evaluate the nature and extent of hydrocarbon emission surface features on the MCA; and 3) to test the hypothesis that the crest of the MCA was a small island during the low sea level stand of the late Pleistocene.

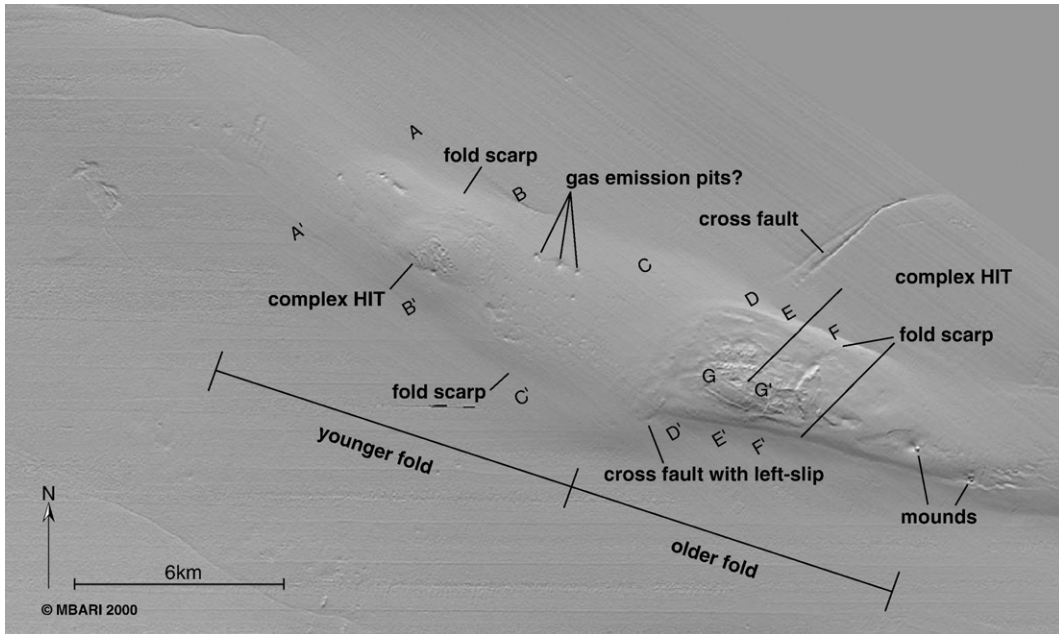


Fig. 2. High-resolution shaded relief view showing geomorphic forms of the Mid-Channel Anticline.

1.3. Approach

In the investigation we have applied geomorphic analysis to: 1) interpret high-resolution topographic

(bathymetric) data in the form of a Digital Elevation Model (DEM), and derivatives including shaded relief views, detailed topographic maps, cross-sections, and profiles along the crest of the MCA; 2) estimate from

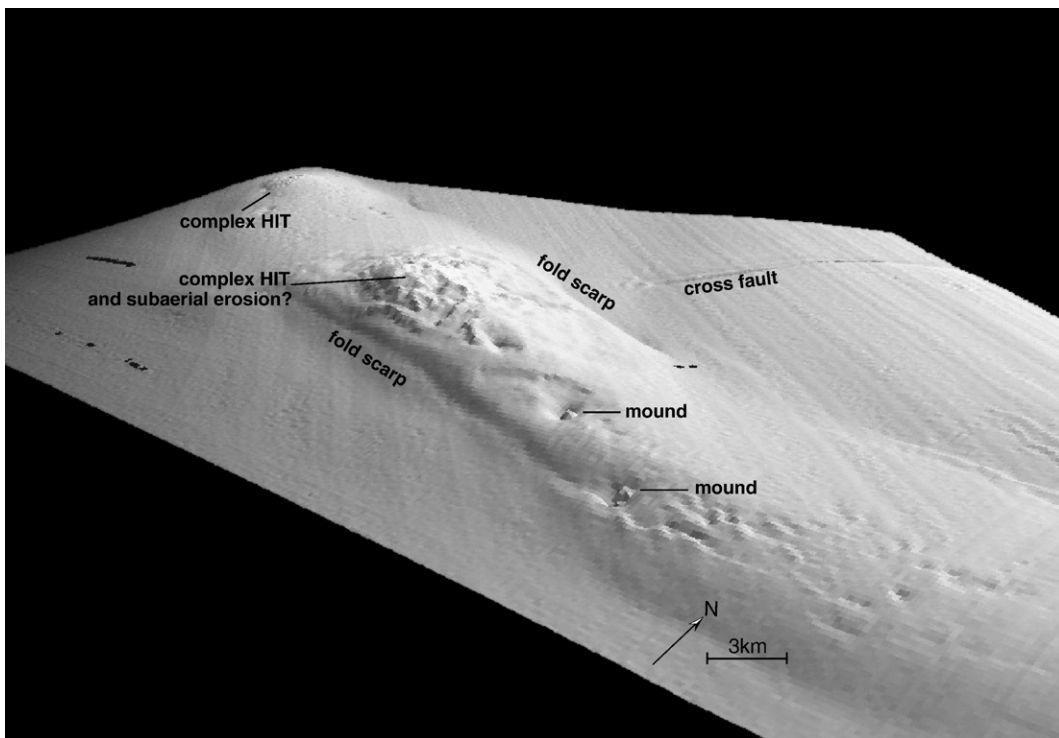


Fig. 3. High-resolution shaded relief (view towards the west) of the Mid-Channel Anticline showing geomorphic features.

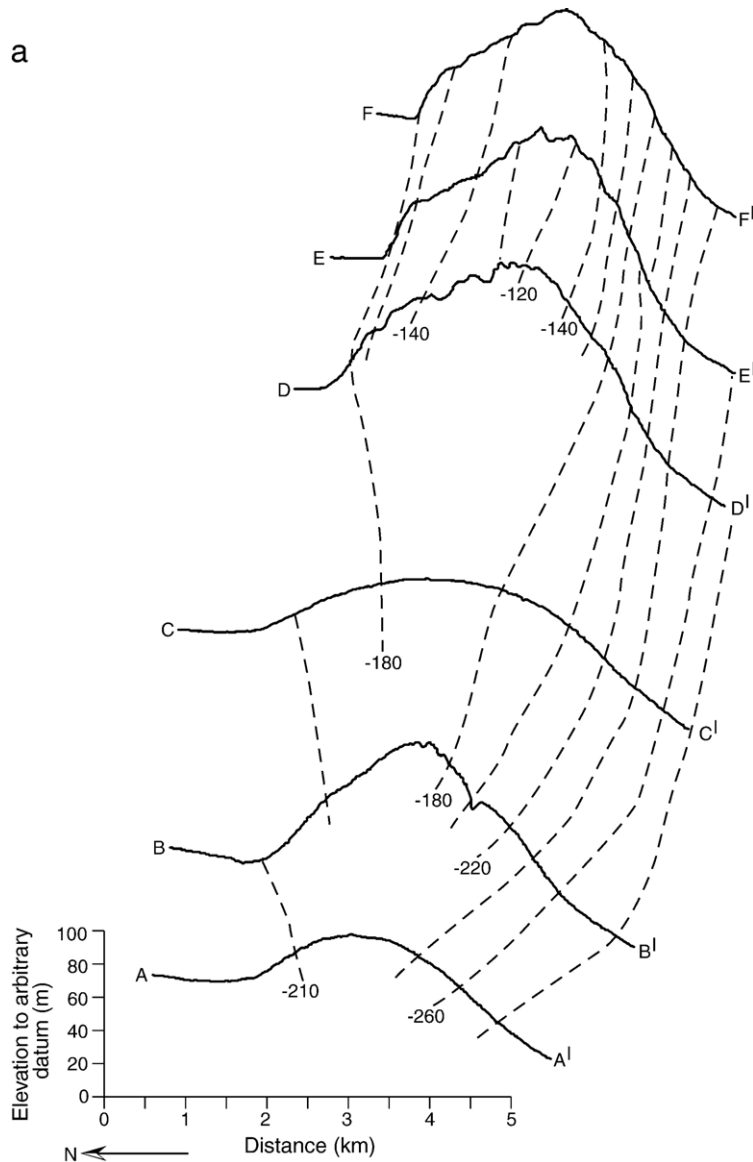


Fig. 4. (a) High-resolution topographic profiles cross the crest of the Mid-Channel Anticline, (VE \sim 25); and (b) topographic profile along part of the crest of the fold (VE \sim 10). Locations of profiles are shown on Fig. 2.

paleo-sea level curves and rates of tectonic movement the position of the crest of MCA at the Last Glacial Maxima (LGM) at 22 to 19 ka; and 3) interpret the geomorphic development of MCA to better understand fold growth.

1.4. Methods

Topographic interpretation of the sea floor at the MCA is based on high-resolution bathymetric and side-scan data collected by the Monterey Bay Aquatic

Research Institute (MBARI) in 1998. Bathymetric data were collected by R/V Ocean Alert using a hull-mounted 300 kHz Simrad EM300 adjustable-angle system with side-scan capability. Shore-based differential GPS allowed locations to be determined with an accuracy of 3 m. Water depth resolution (in depth range of 100 to 200 m) is better than 1 m. Further information concerning the MBARI bathymetric survey of the Santa Barbara Channel is provided by Eichhubl et al. (2002).

Topographic analysis utilizes high-resolution bathymetric data (DEM) coupled with shaded relief views,

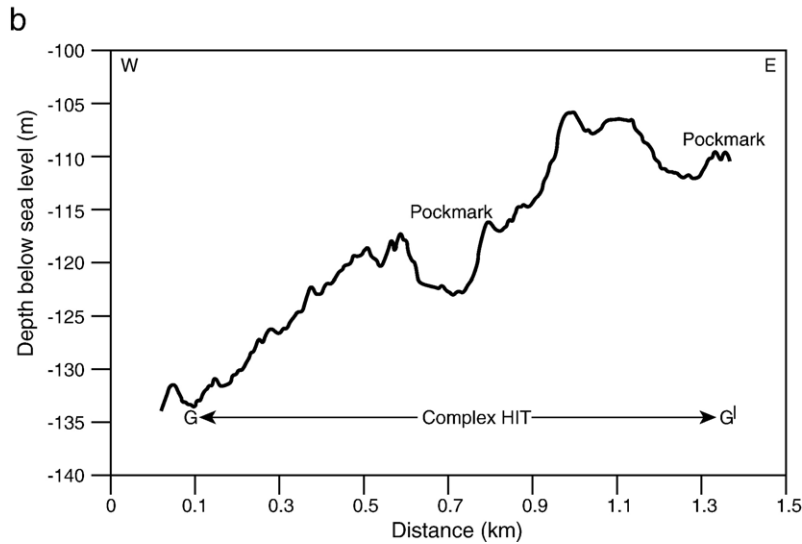


Fig. 4 (continued).

high-resolution topographic maps and cross-sections. These allow detailed evaluation of the subsurface topographic expression of surface features within Santa Barbara Basin.

2. Topographic data

The westernmost 25 km of the structure is a well developed fold. Geomorphic features of the fold are depicted on Figs. 2 and 3, and show steeper topography particularly near the crest of the eastern terminus of the fold. The side slopes of the anticline are only a few degrees, yet are approximately one order of magnitude steeper than the slopes of the sea floor adjacent to the structure. Most of the anticline consists of a relatively smooth surface that is gently folded, forming fold scarps. These scarps are steeper in the eastern part of the fold. The center of the MCA is a topographic saddle that separates the eastern and western parts of the fold.

High-resolution topographic profiles and the shaded relief views provide further details of the fold. Topographic profiles across MCA on Fig. 4a are arranged from west (bottom) to east (top). Dashed lines represent modern water depths with the topographically highest point on profile *E* at a water depth of 105 m. With exception of profile *B*, relief increases from about 40 m to 100 m from west to east. Profiles *A* and *C* are smooth and depict the morphology of the fold with relatively little erosion. Profiles *B* and *D–F* are not nearly so smooth near the crest with local relief of 5 to 10 m. Profiles *A*, *B*, and *D–F* are asymmetric with steep slope on the south. The 1.3 km profile along

part of the crest of MCA (profile *G*) increases in relief by about 30 m from west to east (Fig. 4b). Also present are two depressions about 100 m across and a few meters deep.

3. Interpretation

3.1. Geomorphology

Shaded relief views and the topographic profile along the crest of the MCA suggest there are three segments to the structure (Fig. 5). The easternmost segment apparently ends at a cross fault (Figs. 2 and 3) and we postulate that a similar cross fault may exist at the contact between the central segment and the westernmost segment. Figs. 2 and 3 suggest the cross fault has a component of left-lateral displacement, visible on the southern fold limb as an offset in the fold scarp. The fault on the seabed north of the fold is expressed as a shallow linear groove suggestive of strike-slip with little vertical displacement (Fig. 6). The geomorphic expression appears to be a smaller version of large grooves produced in the landscape by the San Andreas Fault in the Carrizo Plain of Central California (see for example Schultz and Wallace, 1997). The grooves are preserved near MCA because there is little erosion or deposition, and detected because of the high-resolution topographic data. The grooves at MCA are different than those of the San Andreas Fault in that there is no vertical relief across them. The topography east of the assumed cross fault suggests a component of vertical displacement during fold growth.

Based on seismic mapping, Mueller et al. (1994) suggested that the MCA has propagated westward several tens of kilometers during the past 1 My. Tectonic geomorphic expression of the fold also suggests a western propagation of the structure (Keller et al., 1999, 2001). To the west elevation of the crest decreases, side slopes decrease in declivity, topography is generally smoother, and folding was initiated more recently to the west.

In summary, we observe from the geomorphic analysis that: 1) the structure is segmented; 2) a prominent cross fault is a segment boundary; 3) the fold scarps along the MCA are variable with respect to height, width, and steepness; 4) there is some evidence for surface faulting; and 5) MCA is apparently propagating to the west.

3.2. Model of fold growth

A fundamental principle of geomorphology is that a change in form implies a change in process. Minor but potentially significant changes in form of the fold probably reflect changes in tectonic processes. The shaded relief views (Figs. 2 and 3) when coupled with the topographic profiles (Figs. 4 and 5) show that the eastern segment of the fold has steeper, narrower limbs with fold scarps. The cross fault at the western terminus of the eastern segment is close to where the vertical relief of the structure is greatest. This suggests that the eastern segment and blind faults grew laterally as displacement increased (Jackson et al., 1996). The geomorphology indicates that fold growth apparently paused for some period of time as displacement increased, the fold tightened and strain accumulated at the fault tip near the cross fault. The fold then propagated laterally to the west from the cross fault. Lateral propagation led to the development of distinctive topography including the plunge panel observed at the western termination of the topographic expression of the fold (Fig. 2). This mode of fold growth is similar to Wheeler Ridge in the southern

San Joaquin Valley (Mueller and Talling, 1997; Keller et al., 1998) where fold growth propagated laterally by steps with cross faults forming segment boundaries.

3.3. Estimating rates of subsidence

Shortening across Santa Barbara Basin from GPS data near MCA is about 6 mm/yr (Larson and Webb, 1992). Assuming low angle reverse faulting with dip of 10° to 20° (Shaw and Suppe, 1994; Pinter et al., 2003), the regional rate of subsidence (density driven, isostatic response due to crustal thickening) is about 0.8 to 1.6 m/ky. For a fault dip of 10° the calculation is: $\tan 10^\circ (6\text{m/ky}) \left(\frac{2.5 \times 10^3 \text{kg/m}^3}{3.3 \times 10^3 \text{kg/m}^3} \right) = 0.8\text{m/ky}$. The rate of 1.6 m/ky is obtained if the dip of the fault is 20° . We assume the unit mass of the crust of Santa Barbara Basin is $2.5 \times 10^3 \text{kg/m}^3$ (following Pinter et al., 2003) and that of the mantle is $3.3 \times 10^3 \text{kg/m}^3$. This rate of subsidence generally agrees with estimates of Pinter et al. (2003). At Santa Cruz Island, about 20 km south of the MCA, rates of uplift and subsidence are nearly balanced at 0.5 to 0.7 and 0.8 m/ky respectively. Isostatic subsidence at MCA is also a function of thickening, due to shortening north to the Santa Ynez Mountains, and thus a reasonable estimate for subsidence due to total tectonic loading is 0.8 to 1.6 m/ky since the Last Glacial Maximum. Rates of sedimentation on the crest area of the MCA are low (about 0.1 m/ky), and much of the area is late Pleistocene bedrock exposure with little or no modern sediment accumulation (Eichhubl et al., 2002; Hill et al., 2003; Nicholson et al., 2006).

3.4. Hydrocarbon induced topography (HIT)

The Santa Barbara Channel is the location of major oil fields and some of the largest known marine

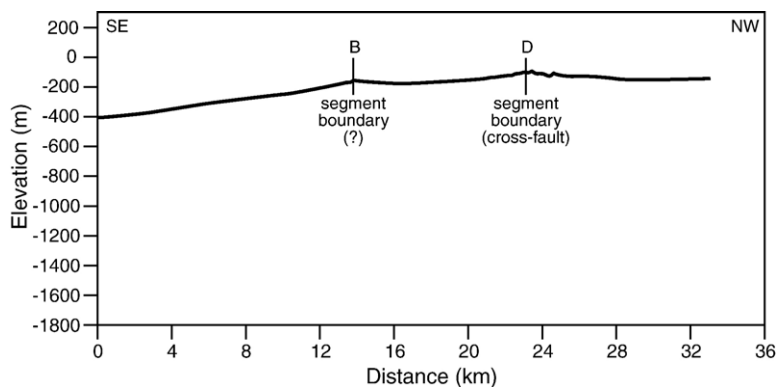
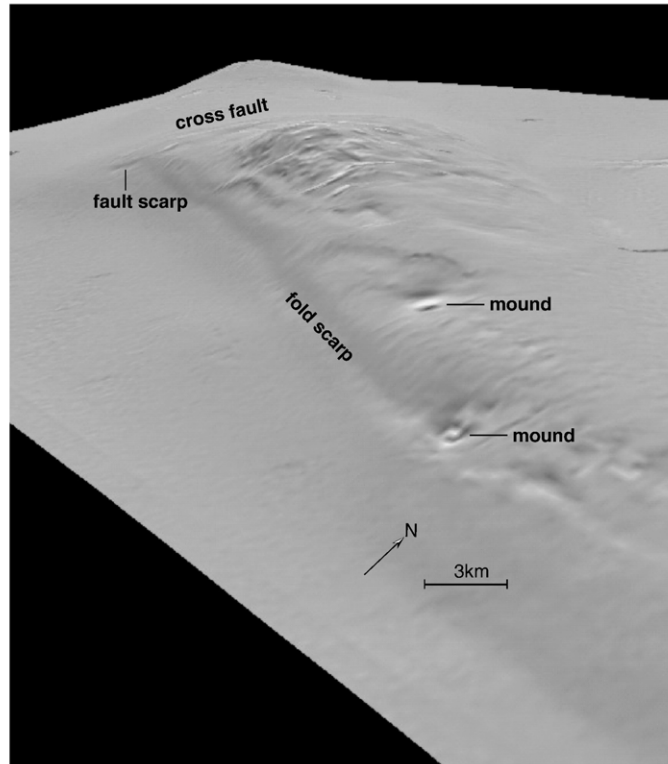


Fig. 5. Topographic profile along the crest of the Mid-Channel Anticline showing apparent segment boundaries.

a



b

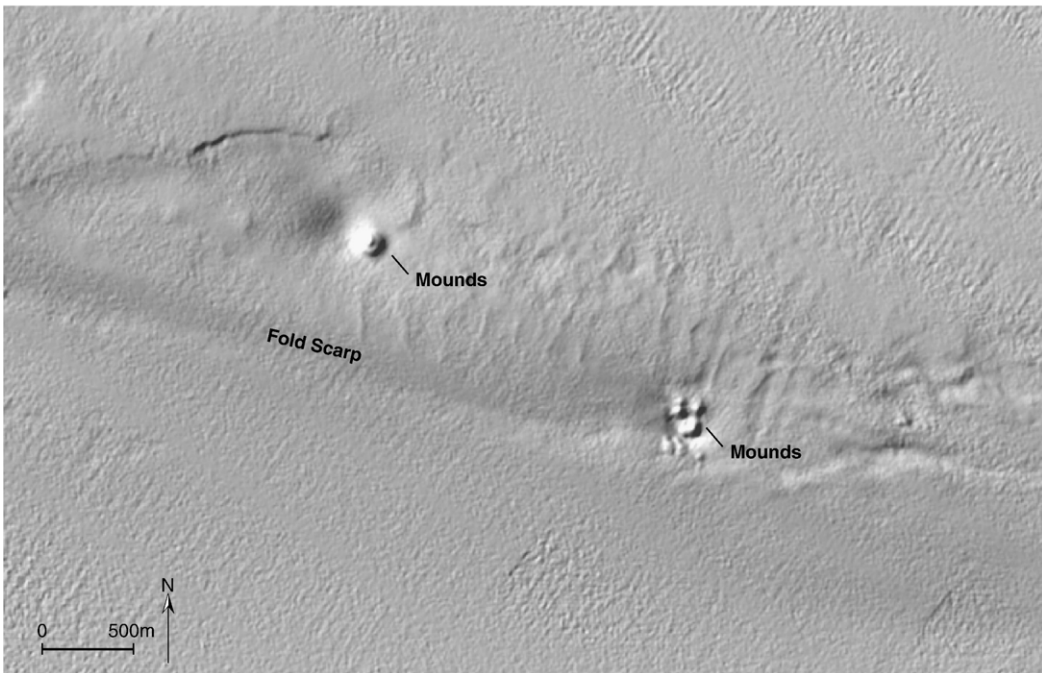


Fig. 6. (a) High-resolution shaded relief view showing mound morphology in relationship to the Mid-Channel Anticline; and (b) details of mound morphology.

hydrocarbon seeps in the world (Hornafius et al., 1999; Eichhubl et al., 2002). Several areas in the basin, including the MCA, have been identified as having hydrocarbon induced topography (HIT), defined as topography particular to and dependent on accumulation or emission of hydrocarbons. HIT including mud volcanoes, mounds and pockmarks is known from many locations around the world (Hovland and Judd, 1988). Based on worldwide identification, Table 1 is a suggested classification of HIT.

Hydrocarbon induced topography at MCA has several forms (see Figs. 2 and 3). Pockmarks range in size from 4 m to over 300 m in diameter with depths from less than 1 m to more than 15 m (resolution for the topographic profiles from the DEM is less than 1 m).

Mounds have diameters of several hundred meters and heights of several tens of meters. Complex HIT topography consisting of the coalescence of pockmarks is also present. The length to width ratio of the pockmarks range from 1.0 to 5.9 and the pockmarks cover a cumulative area of about 1.14 km². Examination of Fig. 2 suggests alignment of pockmarks for the western and central segments of the anticline.

Cores from the crest of the MCA were taken by MBARI. In one pockmark with diameter of about 500 m and depth of several meters, hydrocarbon gas was observed seeping from the pockmark. Based on this observation and that the MCA is in a major petroleum region, we assume the pockmarks and mounds are produced as a result of tectonics and emission of methane,

Table 1
Classification of hydrocarbon induced topography (HIT)

Form	Description	Comments	Examples
Mud volcano ¹	Conical shape from about 100 m to several km across. May be up to several hundred m high	Constructional: found on land and on seabed, produce mud, breccia as explosive deposits or flows (breccia flow); may have self-ignition of methane with flames to heights of several hundred meters.	Azerbaijan, Caspian Sea ^{1,3} Columbia ³ , sea off the southeastern coast of Trinidad ³ ; southwest African continent margin ⁴
Mounds ²	Shield shape from a few m in diameter to a few hundred m. May be a few to several tens of m high; may have central crater	Constructional: seabed forms; some are similar to mud volcanoes with extrusion of gas (mostly methane) and/or tar.	Arabian Gulf ³ ; Santa Barbara Basin; upper Ojai Valley, CA
Mud cone ¹	Small cone with diameter of a few to about 50 m and height of 0.5 to 10 m	Constructional: on land, may have a small crater from which water, mud, tar or gas is released; lacks ejection deposits characteristic of mud volcanoes.	Azerbaijan ¹ ; Carpinteria, California ⁶
Salse ¹	Less developed type of cone, crater at top filled with mixture of mud, gas (mostly methane), water and at time, tar or oil. Diameter from less than 1 m to about 20 m	Constructional: on land, may be circular in shape, may appear as a shallow lake with rising gas bubbles.	Azerbaijan ¹ ; upper Ojai Valley, CA
Gryphones ¹ (seepage hole)	Pit or seepage hole with diameter of a few m to several hundred m and depths of a few m to several tens of m	Erosional: on land, are seepage holes with mixture of oil, gas and/or water.	Azerbaijan ¹ ; La Brea, Los Angeles, California ⁴
Pockmark ^{2,3} (crater, may be elongated)	Steep sided erosional features with diameter of a few m to several hundred m. and depths of a few m. to several tens of m	Erosional seafloor features; some smaller ones may correspond to on land forms such as the gryphone. May be formed by explosive release of gas (mostly methane).	Scotia Shelf ² ; North Sea and many other locations ³ ; Eel River Basin ⁷ ; Santa Barbara Basin ⁸
Crater field	Field of pockmarks or craters	Erosional: Seafloor density in a field may be up to several hundred pockmarks per km ² .	Scotia Shelf ² Eel River Basin ⁷ North Sea ³ Santa Barbara Basin ⁸
Breccia or tar flow	Variable sizes from a few m. to more than 1 km	Constructional or depositional on land or sea floor from mud volcanoes, mounds or salse	Azerbaijan ¹ Santa Barbara Basin; tar flow from sea cliff, Goleta, CA; upper Ojai Valley tar flows, CA
Carbonate mats, crust, mounds or chimneys	Generally small features on the scale of a few cm to a few m	Constructional on seafloor: Formed when methane oxidizes over vents.	Santa Barbara Basin ^{8,9} ; North Sea ³ ; Mediterranean Sea ¹⁰
Complex forms	Mixture of mounds, pockmarks, gryphones, carbonate mats, crust and mounds	Constructional and erosional: Mud volcanoes, pockmarks and mounds and other gas emission features that may coalesce in complex ways.	Santa Barbara Basin ⁹

¹Aliyev et al. (2002). ²King and MacLean (1978). ³Hovland and Judd (1988). ⁴Ben-Avraham et al. (2002). ⁵Stock (1992). ⁶Arnold (1907). ⁷Yun et al. (1999). ⁸Eichhubl et al. (2002). ⁹Boles et al. (2001). ¹⁰Coleman and Ballard (2001).

oil, and tar. Small pockmarks and tar mounds have been known to form just offshore of Coal Oil Point located about 20 km northwest of the study site on the MCA (Leifer et al., 2004).

Two AMS radiocarbon dates from cores taken in the pockmarks on the MCA provide calibrated dates of 25.3 ka and 36.9 ka for depths in the core of about 1 cm and 14 cm, respectively (Hill et al., 2003). Planktonic foraminiferal biostratigraphy in this core is consistent with sediments of glacial age (oxygen isotope stage 3). Thus, the pockmarks formed prior to ~37 ka, with an unconformity or winnowing in the sediments after 25 ka (hence, no modern sedimentation). Sea level at 37 ka was about 70 m lower than today. This suggests that HIT at the MCA formed at shallower water depth and lower water pressure than today. Alternatively, the pockmark may have formed more recently, with sediment displacement associated with this process accounting for the lack of Holocene sedimentation.

The formation of the complex hydrocarbon induced topography at MCA evidently has experienced sufficient erosion that postglacial sediments are not present in the area. Lack of sediment is also suggested by the high backscatter data collected by MBARI delineating the prominent exposure of bedrock along portions of the MCA (Eichhubl et al., 2002).

Two areas of complex hydrocarbon induced topography along the anticline are evident (Figs. 2 and 3). One is in the eastern area of the fold and another is ~8 km to the west. The topographic expression of the HIT at the eastern site is much more pronounced in part because it was likely exposed to subaerial erosion during the Pleistocene sea level lowstand (corresponding to LGM) at about 20 ka. The topography to the west was probably not exposed, as the deeper water

depths of about 160 m likely precluded subaerial exposure during the LGM.

The surface of the anticline is generally smooth. However, where the complex HIT is present the topography has variable relief due to the abundance of pockmark depressions and their coalescence to form erosional topography. The areas with greatest roughness at the MCA are above a depth of 140 m, and probably resulted from a combination of HIT development and subaerial erosion.

Several domes ranging in diameter from a few 10 s of meters to more than 100 m are located on the fold scarp of the southern limb of MCA (Figs. 2, 3 and 6). The mounds are within or adjacent to a circular depression. The origin of the mounds is unknown in the absence of direct observations of the ocean floor. However, several possible hypotheses may account for these features: 1) they result from over-pressurization in the upper rocks and surface sediments leading to doming of the sea floor; 2) they were produced by tar extrusion producing tar mounds on the ocean floor (Fig. 7); 3) they are sediment accumulations resulting from gas emissions from the ocean floor; or 4) they are composed of drilling waste from exploratory drilling. The last explanation seems unlikely because, following a search of records of drilling activity, no drilling was recorded in the immediate vicinity of the mounds (Munger, 2001). Further, features >100 m in diameter are too large to be drilling waste. Geomorphic support for the hypothesis that the larger domes are the result of over-pressurization, similar to that of the Ventura Avenue Anticline about 25 km to the east (Yeats, 1983), is suggested by the similarity in size of the domes with large pockmarks. We suggest that some of the domes may initially develop as a small mound and then burst to become pockmarks.

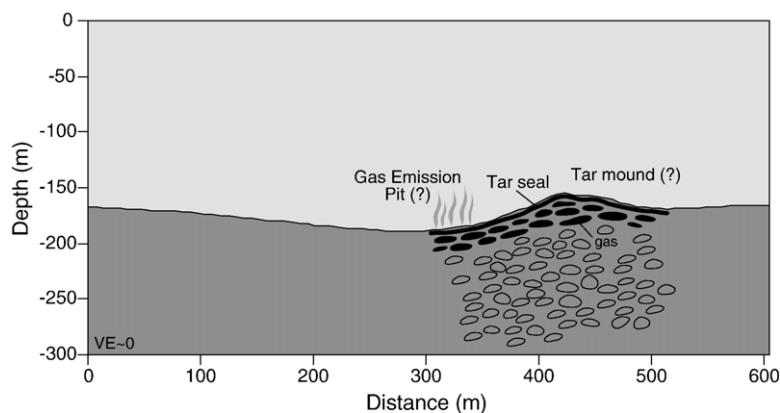


Fig. 7. Topographic profile of the large west mound of Fig. 6. The interpretation of tar mounds with emission of hydrocarbon gases is hypothetical.

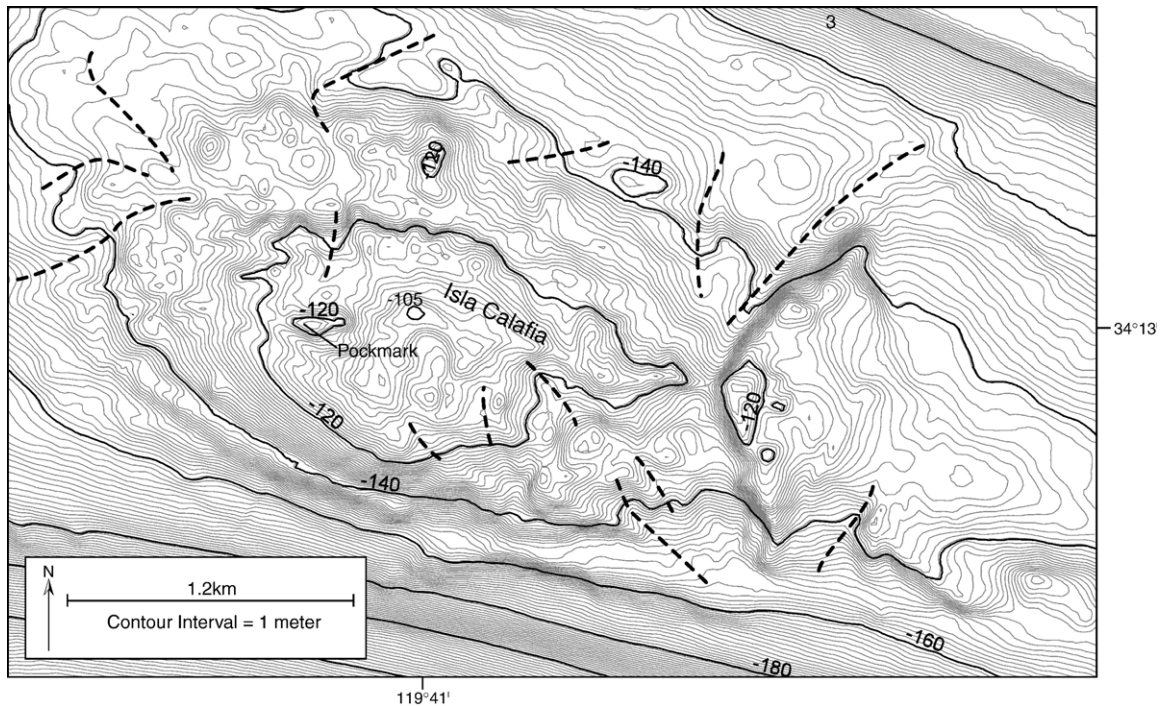


Fig. 8. Topographic map with (contour interval) of 1 m for the crestal area of the Mid-Channel Anticline. The relatively rough topography compared to that found on the bottom of the Santa Barbara Basin suggests that the area above approximately -140 m was probably eroded in part from surface processes during the Last Glacial Maximum (LGM) about 20 ka. Possible channels that drained the area are shown as dashed lines.

3.5. Evidence for a late Pleistocene Island

We present the hypothesis that the summit of MCA formed a small island named Isla Calafia (Keller et al., 2001) during the Pleistocene low sea level stand at about 20 ka. The rough topography of the summit area suggests surface erosion above sea level. The 1 m contour interval map (Fig. 8) and shaded relief views (Figs. 2 and 3) above a water depth of about 130 m exhibits several erosional features that may be short channels or gullies. This topography is interpreted to be evidence for subaerial erosion.

Using various possible rates of tectonic processes, and subsidence due to isostatic response to crustal thickening we can estimate the elevation of the high point of MCA during the late Pleistocene low stand using the equation:

$$E_{20ka} = Wd_{20ka} - Wd_p - U_{20ka} + S_{20ka}$$

Where $E_{20 ka}$ is elevation with respect to sea level at LGM, 20 ka; $Wd_{20 ka}$ is sea level change from present to 20 ka, about 120 m but perhaps as much as 130 to 135 m with isostatic adjustment due to 120 m of seawater (Yokoyama et al., 2000; Keller and Pinter 2002); Wd_p is present depth to summit area (105 m); $U_{20 ka}$ is uplift

during last 20 ky; and $S_{20 ka}$ is subsidence of summit area during the last 20 ky. These results are summarized in Table 2 for nearly all reasonable combinations of uplift and subsidence. This analysis suggests that the summit area of the MCA was a late Pleistocene island.

Table 2
Estimated elevation of the summit area of the Mid-Channel Anticline relative to sea level at 20 ka ($E_{20 ka}$) with variable rates of uplift (U) and subsidence (S)

Uplift rate (m/ky) ^a	$E_{20 ka}$; assuming S of 0.8 m/ky ^b	$E_{20 ka}$; assuming S of 1.6 m/ky
0.2	27(37)	43(53)
0.5	21(31)	37(47)
1.0	11(21)	27(37)
1.5	1(11)	17(27)
2.0	-9(1)	7(17)

Present elevation of summit area is -105 m. Assuming sea level at 20 ka was -120 m, equation used is: $E_{20 ka} = Wd_{20 ka} - Wd_p - U_{20 ka} + S_{20 ka}$ where $E_{20 ka}$ is elevation of summit area with respect to sea level at 20 ka; $Wd_{20 ka}$ is sea level change from present to 20 ka (120 m); Wd_p is present depth to summit area (105 m); $U_{20 ka}$ is uplift during last 20 ky; and $S_{20 ka}$ is subsidence of the summit area during last 20 ky due to tectonic loading. $E_{20 ka}$ in parenthesis assumes sea level at 20 ka was -130 m.

^a Vertical rate of faulting 0.1 to 0.2 m/ky, and vertical rate of growth of structural relief is 1.0 to 1.5 m/ky.

^b Most conservative estimate.

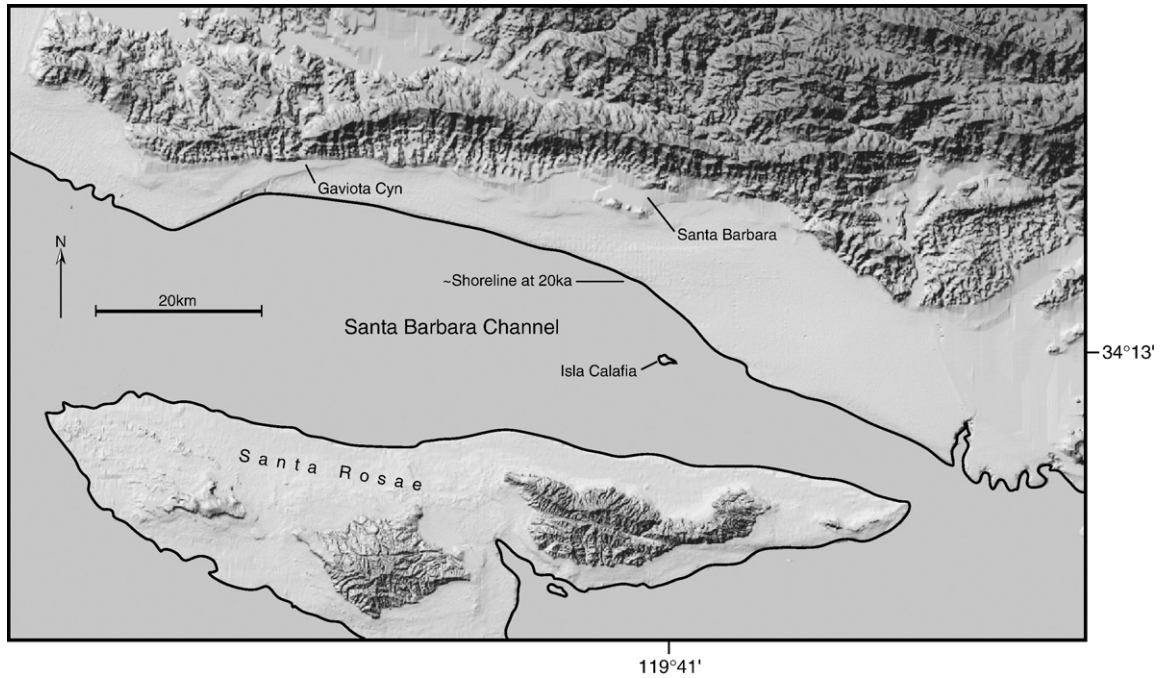


Fig. 9. Map of the Santa Barbara Basin as it may have appeared during the Last Glacial Maxima (LGM) about 20 ka. At that time, the major Channel Islands were one large structure known as Santa Rosa Island Calafia was smaller than Anacapa Island today and was located several kilometers from the mainland LGM shoreline.

Fig. 9 shows the paleo-shoreline at the LGM for the Santa Barbara Channel. As sea level rose rapidly during deglaciation and covered Isla Calafia, it was not flattened by wave erosion. Initial sea level rise at ~15 ka was ~1 cm/yr, evidently rapid enough to preserve the topography.

Another area of rough hydrocarbon induced topography at present water depth of ~160 m is near the west end of the MCA (Figs. 2 and 3). In spite of greater water depth, the origin of the HIT may have resulted from subaerial erosion. Subaerial erosion is possible if the total rate of subsidence due to tectonics and seawater loading

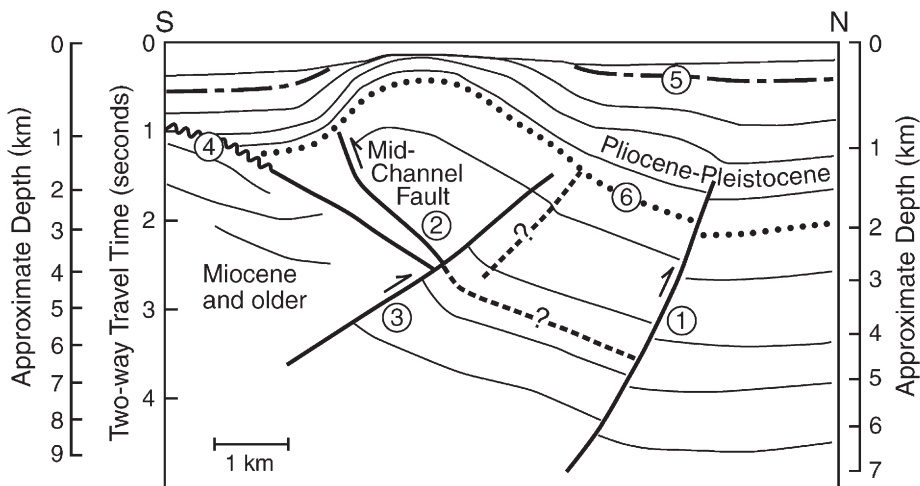


Fig. 10. Simplified geologic section across the Mid-Channel Anticline at the location of E–E' on Fig. 2. Most of the folding at this location results from displacement on the Mid-Channel Fault, and the fold verges south. Circled numbers are: 1, Oak Ridge Fault; 2, Mid-Channel Fault; 3, Unnamed fault; 4, unconformity between Miocene and older rocks; 5, Stratigraphic marker ODP893 at 110 ka; and 6, Stratigraphic marker of 1 Ma (Yeats, 1981). Modified after drawing provided by C. Sorlein (personal written correspondence) and Nicholson et al. (2006).

was 1.6 m/ky, uplift was very low and sea level at 20 ka was lower by 135 m. Assuming MCA is propagating towards the west, as suggested by the geomorphology, the younger western part of the fold would have experienced a lower rate of uplift during the last 1 Ma, than the more eastern part. The rough topography is not nearly so pronounced as at the summit and may be due mostly to emission of hydrocarbon gases.

4. Discussion

Geomorphic interpretation of the topography of the MCA has resulted in better understanding of the structural development of the fold. This approach uses the geomorphology to assist or complement structural interpretation rather than only using subsurface geological and geophysical data to interpret the geomorphology (See Keller et al., 1998; Keller and Pinter, 2002). A recent structural interpretation of MCA, based on high-resolution multichannel seismic reflection and single-channel data linked with stratigraphic correlation with well data (Nicholson et al., 2006) is shown in Fig. 10. This interpretation emphasizes the role of fault-related folding. The anticline was breached by erosion during the last 110 ky. Notice the 110 ka horizon of Nicholson et al. (2006) and the 1 Ma horizon of Yeats (1981) are displaced by both the Oak Ridge and Mid-Channel Faults. These faults have several hundred meters of displacement and reach within 1.5 km of the surface. The important point here is the presence of near-surface faulting. The interplay between displacement on both the Oak Ridge Fault and Mid-Channel Fault produce the observed active anticline. The breaching of the MCA shown on Fig. 10 suggests with reconstruction of the 110 ka surface over the fold, that several hundred meters of rock must have been removed from the summit. This supports the argument for erosion of the summit by wave action and running water.

Geomorphic data emphasize folding; the limbs of the fold steepened to form fold scarps on both limbs (Figs. 2 and 3). The crest of MCA is geomorphically and structurally segmented; a cross fault deforms both the ocean floor south of MCA and cuts across the fold (Figs. 2 and 3). The geomorphic data support the hypothesis of active folding and near-surface faulting at MCA.

5. Conclusions

The most western sector of the Mid-Channel Anticline (MCA) is an actively growing fold with fold scarps and cross faults that segment the structure.

At the MCA in Santa Barbara Basin, complex hydrocarbon induced topography (HIT) exists in several locations. The dominant forms include pockmarks and domes, which vary in size from about 10 m in diameter to over 300 m in diameter. The pockmarks are several meters deep and relative relief of the largest domes is several tens of meters. Analysis of the complex topography on the MCA suggests that at the crest of the structure the topography developed in part as a result of erosion from emission of hydrocarbon gases that formed pockmarks. Consideration of the breached anticline (see Fig. 10) suggests that several hundreds of meters of rock have been removed from the summit of the MCA, suggesting erosion by waves is likely to have occurred.

Vertical rates of faulting and rock uplift due to folding linked with density driven subsidence and sea level at 20 ka, suggest the summit of the MCA was a small late Pleistocene island during the Last Glacial Maximum.

Acknowledgements

This project was supported in part by National Science Foundation grant EAR-9803115. Bathymetry was provided H.G. Green and Peter Eichhubl through the Monterey Bay Aquatic Research Institute. Reviews and suggestions for improvement by Christopher Sorlien, Arthur Sylvester, Robert Yeats, and two anonymous reviewers for *Geomorphology* are appreciated.

References

- Aliyev, A., Guliyev, I.S., Belov, I.S., 2002. Catalogue of recorded eruptions and mud volcanoes of Azerbaijan. Nafta-Press, Baku. 87 pp.
- Arnold, R., 1907. Geology and oil resources of the Summerland District. U.S. Geological Survey Bulletin, vol. 321. 67 pp.
- Ben-Avraham, Z., Smith, G., Reshef, M., Jungslager, E., 2002. Gas hydrate and mud volcanoes on the southwest African Continental margin off South Africa. *Geology* 30, 927–930.
- Boles, J.R., Clark, J.F., Leifer, I., Washburn, L., 2001. Temporal variation in natural methane seep rate due to tides, Coal Oil Point area, California. *Journal of Geophysical Research* 106 (11), 27077–27086.
- Coleman, D.F., Ballard, R.D., 2001. A highly concentrated region of cold hydrocarbon seeps in the southeastern Mediterranean. *Geo-Marine Letters* 21, 162–167.
- Crowell, J.C., 1987. Late Cenozoic basins of onshore Southern California: complexity is the hallmark of their tectonic history. In: Ingersoll, R.V., Ernst, W.G. (Eds.), *Cenozoic Basin Development of Coastal California*. Prentice Hall, Englewood Cliffs, pp. 207–241.
- Eichhubl, P., Greene, H.G., Maher, N., 2002. Physiography of an active transpressive margin basin; high-resolution bathymetry of the Santa Barbara Basin, Southern California continental borderland. *Marine Geology* 184 (1–2), 95–120.
- Gurrola, L.D., Keller, E.A., 1997. Tectonic geomorphology of the Santa Barbara fold belt, western Transverse Ranges, California. *GSA Abstracts with Programs* 29 (6), 344–345.

- Heney, T.L., Teng, T.L., 1985. Seismic Studies of the Dos Cuadras and Beta Offshore Oil Fields, Southern California OCS. Department of the Interior Minerals Management Service, Camarillo, CA.
- Hill, T.M., Kennett, J.P., Spero, H.J., 2003. Foraminifera as indicators of methane rich environments: a study of modern methane seeps in Santa Barbara Channel, California. *Marine Micropaleontology* 49, 123–138.
- Hornafius, J.S., Quigley, D., Luyendyk, B., 1999. The world's most spectacular marine hydrocarbon seeps (Coal Oil Point, Santa Barbara Channel, California): quantification of emissions. *Journal of Geophysical Research* 104 (C9), 20,703–20,711.
- Hovland, M., Judd, A.G., 1988. Sealed pockmarks and seepages: Impact on geology, biology and the marine environment. Grum and Trotman, London. 293 pp.
- Jackson, J., Norris, R., Youngson, J., 1996. The structural evolution of active fault and fold systems in central Otago, New Zealand; evidence revealed by drainage patterns. *Journal of Structural Geology* 18 (2–3), 217–234.
- Keller, E.A., Gurrola, L.D., 2000. Earthquake Hazard of the Santa Barbara Fold Belt, California. Final report for NEHRP Award #99HQGR0081.
- Keller, E., Loaiciga, H., 1993. Fluid-pressure induced seismicity at regional scales. *Geophysical Research Letters* 20 (16), 1683–1686.
- Keller, E.A., Pinter, N., 2002. *Active Tectonics*. 2nd ed. Prentice Hall, Upper Saddle Rivers. 363 pp.
- Keller, E.A., Zepeda, R.L., Rockwell, T.K., Ku, T.L., Dinklage, W.S., 1998. Active tectonics at Wheeler Ridge, Southern San Joaquin Valley, California. *Geological Society of America Bulletin* 110, 298–310.
- Keller, E.A., Gurrola, L., Tierney, T.E., 1999. Geomorphic criteria to determine direction and rate of lateral propagation of reverse faulting and folding. *Geology* 27, 515–518.
- Keller, E., Kamerling, M., Eichhubl, P., Hill, T., Kennett, J., 2001. Isla Calafia, the fifth Santa Barbara Channel Island? Abstracts with Programs — Geological Society of America 33 (6), 70.
- King, L.H., MacLean, B., 1978. Pockmarks on the Scotian Shelf. *Geological Society of America Bulletin* 81, 3141–3148.
- Larson, K.M., Webb, F.H., 1992. Deformation in the Santa Barbara Channel from GPS measurements 1987–1991. *Geophysical News Letters* 19 (14), 1491–1494.
- Leifer, I., Boles, J.R., Luyendyk, B.P., Clark, J.F., 2004. Transient discharges from marine hydrocarbon seeps: spatial and temporal variability. *Environmental Geology* 46, 1038–1052.
- Mueller, K., Talling, P., 1997. Geomorphic evidence for tear faults accommodating lateral propagation of an active fault-bend fold, Wheeler Ridge, California. *Journal of Structural Geology* 19 (3–4), 397–411.
- Mueller, K., Price, M., Shaw, J., Suppe, J., 1994. Forty-six kilometer westward lateral propagation of the Channel Islands Thrust in the last 1 Ma revealed by axial surface mapping, Santa Barbara Channel, California. *AAPG Bulletin* 78 (4), 671.
- Munger, 2001. Map Book, California-Alaska Oil and Gas Fields.
- Namson, J., Davis, T., 1988. Structural transect of the western Transverse Ranges, California; implications for lithospheric kinematics and seismic risk evaluation. *Geology* 15 (8), 675–679.
- Nicholson, C., Kennett, J., Sorlien, C., Hopkins, S., Behl, R., Normark, W., Sliter, R., Hill, T., Pak, D., Schimmelmann, A., Cannariato, K., SB Core team, 2006. Extending the high-resolution global climate record in Santa Barbara Basin. *Eos (Transactions of the American Geophysical Union)* 87 (21), 205–208.
- Pinter, N., Sorlien, C., Scott, A.T., 2003. Fault-related fold growth and isostatic subsidence, California Channel Islands. *American Journal of Science* 303, 300–318.
- Schultz, S.S., Wallace, R.E., 1997. The San Andreas Fault. Accessed 3–18–05 @ <http://pubs.usgs.gov>.
- Seeber, L., Sorlien, C., 2000. Listric thrusts in the western Transverse Ranges, California. *GSA Bulletin* 112 (7), 1067–1079.
- Shaw, J., Suppe, J., 1994. Active faulting and growth folding in the eastern Santa Barbara Channel, California. *Geological Society of America Bulletin* 106, 607–626.
- Sorlien, C., Kamerling, M., 1998. Fault displacement and fold contraction estimated by unfolding of Quaternary strata, onshore and offshore in the Ventura basin, California. Final report to US Geological Survey, NEHRP, Contract 97GR 03085.
- Sorlien, C., Gratier, J.P., Luyendyk, B., Hornafius, J.S., Hops, T.E., 2000. Map restoration of folded and faulted late Cenozoic strata across the Oak Ridge fault, onshore and offshore Ventura basin, California. *GSA Bulletin* 112 (7), 1080–1090.
- Stock, C., 1992. *Rancho La Brea*. 7th ed revised by J.M. Harris. No. 37, Science Series. Natural History Museum of Los Angeles County. 113 pp.
- Sylvester, A., Smith, S., Scholz, C., 1970. Earthquake swarm in the Santa Barbara channel, California, 1968. *Bulletin of the Seismological Society of America* 60 (4), 1047–1060.
- Yeats, R.S., 1981. Quaternary detachment structures in Ventura Basin, Southern California. *Eos, Transactions of the American Geophysical Union* 62 (17), 398.
- Yeats, R.S., 1983. Large-scale Quaternary detachments in Ventura Basin, Southern California. *Journal of Geophysical Research* B 88 (1), 569–583.
- Yokoyama, Y., Lambeck, K., DeDeckker, P., Johnston, P., 2000. Timing of the last glacial maxima from observed sea-level minima. *Nature* 406, 713–716.
- Yun, J.W., Orange, D.L., Field, M.E., 1999. Subsurface gas offshore of Northern California and its link to submarine geomorphology. *Marine Geology* 154, 357–368.